Norwegian University
of Life Sciences

Master's Thesis 2016 60 ECTS
Department of Chemistry, Biotechnology and Food Science

Establishment and Characterization of a Gatekeeper Mutation for Protein Kinase D1 and 3

Maria Xepapadakis Isaksen
Chemistry and Biotechnology: Molecular Biology

Acknowledgements

This thesis was carried out from July 2015 to May 2016 at the Biotechnology Centre of Oslo under the supervision of Group Leader Dr. Michael Leitges, on behalf of the Norwegian University of Life Sciences, Department of Chemistry, Biotechnology and Food Science.

First and foremost, I would like to express my deepest gratitude towards Dr. Michael Leitges for all his guidance and help in the completion of this thesis. Your patience and scientific expertise has been deeply appreciated.

I would also like to thank the group engineer Ursula Braun for all the technical assistance, training and company in the lab. Your technical experience has been invaluable in resolving any obstacles that have occurred throughout the practical work.

In addition, I would like to thank Dr. Tianzhou Zhang for taking the time to assist me with technical operations and data analysis. I would also like to thank you for all the discussions and the company during late working hours.

Lastly, I would like to thank the group all together for welcoming me and supporting me through this whole process. This has without doubt been the most exciting and educational project I have been a part of, and I have all you to thank for that.

Oslo, May 2016

Maria Xepapadakis Isaksen

Abstract

Protein kinase D constitutes a novel family of Ser/Thr specific kinases and contains three members; PKD1-3. This protein kinase family has been described to carry out different functions and responses at various locations in the cell through a novel PKC/PKD signal transduction pathway. PKD1 has been reported as a major regulator of ROS mediated signaling, where PKD1 deficiency results in an increased sensitivity to ROS. PKD3 has been reported to be involved in cell cycle regulation, and depletion of PKD3 results in cell cycle malfunction. Due to high homology among the PKDs, it is difficult to identify isoform specific functions. To circumvent this problem an approach termed Analog Sensitive Kinase Technology, developed by Kevan Shokat and his team, can be applied. By mutating the gatekeeper residue within the ATP binding pocket to a residue bearing a smaller side chain, a novel pocket is created within the ATP binding site, that is not found in the wild type kinase. This opens up the possibility for isoform specific inhibition, by using a designed inhibitor (1-Na PP1).

Through a Lenti-virus based expression system, gatekeeper variants of PKD1 and PKD3 were introduced into corresponding deficient cell lines. The introduction of PKD1 gatekeeper variants in PKD1 deficient background, restored PKD1 activity and rescued the deficiency, while the application of the inhibitor restored the cells sensitivity to ROS.

The established cell line expressing exogenous PKD3 gatekeeper variant had a low expression but was able to restore normal cell cycle. However, the application of the 1-Na PP1 resulted in cell cycle malfunction, but the failure was not as significant as recorded for $PKD3^{-/-}$, therefore representing a suboptimal result. Thus we have successfully established stable $PKD1^{-/-}$ cell lines expressing exogenous PKD1 gatekeeper variants that are sensitive to 1-Na PP1 inhibition, but a further experimental evaluation is needed for the $PKD3^{-/-}$ cell lines expressing exogenous PKD3 gatekeeper variant.

Sammendrag

Protein kinase D konstituerer en familie av Ser/Thr spesifikke kinaser og har tre medlemmer: PKD1-3. Denne protein kinase familien er involvert i forskjellige funksjoner og responser på diverse lokasjoner i en celle, gjennom en PKC/PKD signal transduksjon. PKD1 har vært rapportert som hovedregulator av ROS-mediert signalisering, hvor PKD1 mangel resulterer i økt sensitivitet til ROS. PKD3 har vært rapportert å være involvert i cellesyklus regulering, hvor PKD3 mangel fører til defekt i cellesyklusen. Det er høy homologi blant PKD familiemedlemmene, som gjør det vanskelig å identifisere isoform spesifikke funksjoner. For å overkomme dette problemet, kan en tilnærming kalt Analog Sensitiv Kinase Teknologi, utviklet av Kevan Shokat og hans team, bli applisert. En mutasjon av *gatekeeper*-residuet i ATP bindingssetet til en residu med en mindre sidekjede, vil lage en ny lomme på innsiden av ATP bindingssetet som ikke er funnet i vill-type kinasen, og vil derfor tillate isoform spesifikk inhibering ved bruk av en konstruert inhibitor (PP1 analog).

Gjennom et Lenti-virus basert ekspresjonssystem, var gatekeeper varianter av PKD1 og PKD3 introdusert til tilhørende kinase-manglende cellelinjer ($PKD1^{-/-}$ og $PKD3^{-/-}$). Introduksjonen av PKD1 gatekeeper-varianter i $PKD1^{-/-}$, gjenopprettet PKD1 aktivitet og reddet de PKD1 manglende cellene. Ved tilføring av inhibitoren responderte cellene som $PKD1^{-/-}$ og var derfor sensitive mot ROS. Den etablerte cellelinjen som uttrykte eksogene PKD3 gatekeeper-varianter hadde lav ekspresjon, men klarte likevel å gjenopprette normal cellesyklus. Senere amplifisering av inhibitor resulterte i reduksjon av den normale cellesyklusen, men tapet var ikke like signifikant som forutsett. Dermed har vi lyktes med å etablere stabile $PKD1^{-/-}$ cellelinjer som uttrykker eksogene PKD1 gatekeeper-varianter, som er sensitive til PP1 analog inhibering. Videre eksperimentell evaluering er nødvendig for å konkludere responsen til $PKD3^{-/-}$ cellelinjene som uttrykker eksogent PKD3 gatekeeper-varianter.

Innholdsfortegnelse

1 Introduction

1.1 Protein Kinases

Almost all processes that take place within cells require catalysis because the spontaneous reaction rate are far to slow to support normal cellular activity and survival. To do so, specialized proteins exists that fulfill these important roles of catalyzing the biochemical reactions within a cell (Boyer, 1998). A subgroup of such, called protein kinases, can regulate the activity of other proteins (substrates) by transferring a phosphate group onto specific amino acid residues within these substrates. This as phosphorylation described reaction, uses either adenosine triphosphate (ATP) or guanosine triphosphate (GTP) as phospho donor, thus kinases are divided into ATP or GTP specific ones in the first place (Rubin and Rosen, 1975).

Furthermore, kinases are subdivided with regard to their amino acid specificity, which either can be a tyrosine (Tyr), serine (Ser) or threonine (Thr), from which Ser/Thr specific kinases are most abundant. Notably, a few kinases have been reported to be dual specific, phosphorylating both Tyr as well as Ser/Thr residues, but also histidine specific kinases have been reported (Lindberg et al., 1992).

Overall, protein kinases constitute one of the largest and most diverse gene families. The human protein kinase gene family consists of 518 members from which 50 are described as pseudo-kinases since they lack important functional residues within the catalytic domain (Roskoski, 2015). Since protein kinases are predicted as key regulators of almost all cellular functions, it is crucial to distinguish and characterize individual kinase-specific *in vivo* functions.

In general, protein kinases exist in a basal or primed state (not activated) in a cell and become activated only after specific stimulation, which generates specific regulatory stimuli (activators). Such stimulations can arise by binding of external signals molecules, such as growth factors and hormones, to specific receptors on the surface of the target cell (Tuteja, 2009). This binding induces a so-called signal transduction, which eventually transmit a signal from the outside into the cell where it for example can induce gene transcription within the nucleus.

As one of the first kinases identified and characterized, protein kinase A (PKA) was shown to represent a Ser/Thr specific kinase which depends on cyclic AMP (cAMP) (Gill and Garren, 1970). Its solved structure served for a long time as a general model for Ser/Thr kinases, providing evidences of how kinases work mechanistically (Roskoski, 2015). In the inactive state, PKA exists as tetramers composed of two catalytic subunits (C) and two regulatory subunits (R). When cAMP is generated by adenylyl cyclases through G-coupled transmembrane receptor activation, cAMP levels are increasing within the cytosol. This

increase causes cAMP binding to both R subunits, which subsequently leads to the release of the two C subunits, which represents the active part of PKA. Therefore, PKA is one classical example of a kinase regulated by the generation of a second-messenger.

1.2 Protein Kinase C

1.2.1 Introduction to PKC

Protein kinase C (PKC) was identified as second Ser/Thr specific kinase in 1977, distinguished by its dependency on phospholipid and Ca^{2+} binding as prerequisite for its activation (Inoue et al., 1977, Takai et al., 1977). Within a decade of intense research, it was shown that PKC represents a closely related kinase family consisting of at least 11 members with structural similarities. Based on regulatory, structural and enzymatic differences among these isoforms, they are further divided into three subgroups; classical-, novel- and atypical PKC (Ohno and Nishizuka, 2002). All three subgroups comprise a highly conserved C-terminal kinase domain whereas most of the variation between the subgroups occurs in the regulatory domain. In general, the regulatory domain includes a self-inhibitory region termed pseudosubstrate motif (PS), a constant domain 1 (C1, either as tandem repeat or single in atypical PKCs) and a constant domain 2 (C2) or a PB1 (Phox and Bem1p) domain in the atypical PKCs (Roffey et al., 2009). The C1 domain interacts with membrane embedded diacylglycerol (DAG) or artificial activator TPA. The C2 domain in classical PKCs binds Ca^{2+}, while in novel PKCs the C2 domain harbors regulatory motifs responsible for protein-protein or protein-lipid interactions (Nishizuka, 1995). The single C1 domain within atypical PKCs fail to bind DAG. In addition, atypical PKCs do not contain a C2 domain, but instead a PB1 domain, which mediates protein-protein interactions as well. In that manner, the novel PKCs are activated by only DAG, classical PKCs require Ca^{2+} in addition to DAG, whereas atypical PKCs don't bind either DAG nor Ca^{2+} thus be subject to a different activation mechanism.

1.2.2 PKC activation

As for PKA, PKC is regulated by a second-messenger. In general, any kind of membrane receptor activation which subsequently leads to an activation of phospholipase C (mostly β and γ isoforms) will generate diacyl-glycerol (DAG) and inositol 1, 4, 5-triphosphat (IP_3) (Asaoka et al., 1992). Membrane located DAG in combination with adapter proteins like RACK drives PKC to its membrane localization where it is activated. In addition, IP_3 releases Ca^{2+} from internal stores which in case for classical PKCs are requested for a full activation. In contrast

atypical PKCs are not responsive neither to DAG nor Ca^{2+} indicating a separate activation mode. One such alternatives are second messengers generated by the phosphoinositide 3-kinase (PI3K) which also get activated by many membrane receptors via ligand binding.

1.3 Protein Kinase D

1.3.1 The discovery of PKD and its link to PKC

In 1994, a novel human Ser/Thr protein kinase gene was discovered which showed a high homology to PKCs. Based on this fact and the way it was discovered, this new member was classified as an atypical PKC and termed PKCμ/PKD in the first place (Johannes et al., 1994). However, shortly after it was discovered that the overall protein structure of the catalytic domain of this new kinase showed fundamental differences to that of PKCs (Rozengurt et al., 1995). In addition, differences in its substrate specificity were also identified, thus it was concluded this new kinase did not represent a new atypical PKC, instead representing a new kinase named PKD. Further examination of PKDs regulation in living cells revealed that phorbol esters, DAG and serum growth factors induced the activation of PKD (Zugaza et al., 1996). Interestingly, the same study also showed that inhibition of (phorbol-ester sensitive) PKC isoforms blocked PKD activation, thus implying that PKD functions downstream of PKCs in a novel yet undiscovered signal transduction pathway.

Today PKD is classified within the Ca^{2+}/calmodulin-dependent protein kinases (CAMKs) group, thus separated from the PKC family which belong to the AGC group. Along with 2 more members, the protein kinase D (PKD) family consist of three members nowadays (Rozengurt et al., 2005).

Within the last decade a number of studies, mainly using PKD1 as representative, have implied that PKD can function downstream of PKC, thereby defining a novel PKC/PKD signal transduction pathway as earlier mentioned (Stafford et al., 2003, Xu et al., 2015). This PKC-PKD pathway has now emerged as a prevalent key signaling mechanism that controls PKD localization, activation and cellular function, and represents a common signaling path for PKC mediated signaling.

As said, PKD represents a novel family of Ser/Thr specific kinases and contains three members; PKD1/PKCμ, PKD2 and PKD3/PKCν. With respect to the overall structure, PKDs can be subdivided into a N-terminal and a C-terminal part whereby the N-terminal contains mainly regulatory functions and the C-terminal represents the catalytic domain. The regulatory N-terminal consists of two cysteine-rich Zn finger regions (C1), that bind DAG and can interact

with phorbol esters as well, followed by an autoinhibitory plecktin homology (PH) domain (Rozengurt et al., 2005). Comparison of the three members reveals highest homology within the catalytic domain and least within the PH domain.

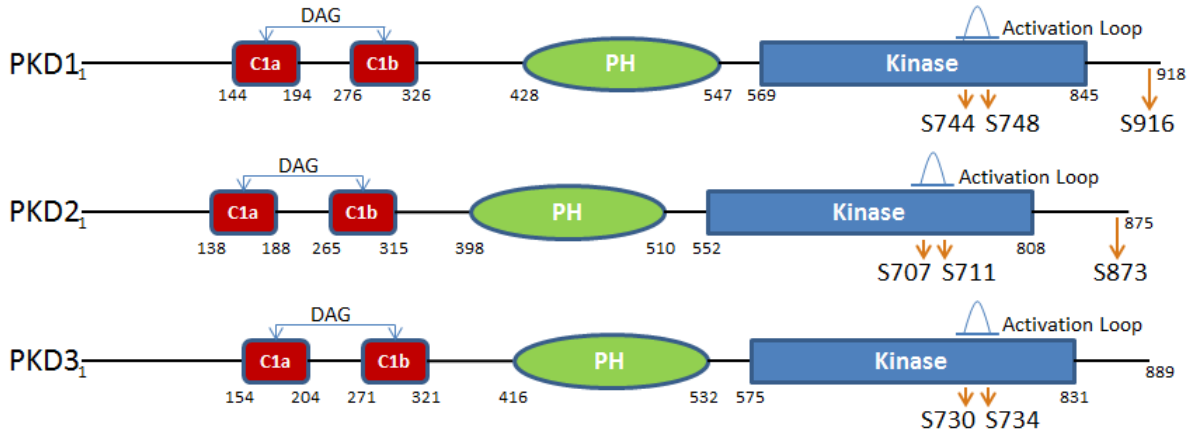

Figure 1. Schematic representation of the mouse PKD isoforms. From N-terminal: DAG binding C1 domains, PH domain and kinase domain. Activation loop (serine (S)) for all isoforms are indicated. In addition, auto-phosphorylation site of PKD1 and PKD2 are also indicated at the C-terminal. Amino acid numbering is represented below each isoform. (Modified from Fu and Rubin (2011) by Leitges group member T. Zhang).

1.3.2 Activation and function of PKD isoforms

Upon a plurality of exogenous cellular stimulations, DAG is subsequently generated and elicits, among other things, a cellular response mediated by PKC/PKD signaling axis. In unstimulated cells, PKDs have been mainly described to be localized in the cytosol and nucleus, but also to a lesser extent in different intracellular compartments (Fu and Rubin, 2011). Once DAG is generated at the membrane, PKD similar to PKC can be recruited to these membranes and interact with DAG via its C1 domain (Wang, 2006). The fact that both kinases translocate to DAG enriched areas enables PKC to interact with and phosphorylate PKD at Ser744/748 (numbering is according to the sequence of PKD1). Ser744/748 represent two critical residues within the activation loop which have been described to be involved in the activation of PKD, thus being accepted as markers for the activation status of PKD. In case of PKD1 and PKD2 this phosphorylation triggers the auto-phosphorylation of a C-terminal serine (Ser916 in PKD1), which also serves as an activation marker. Although some exceptions do exist, this described activation series is known as the general activation mode of all PKDs. Depending on cell context and stimuli, PKDs can integrate signals from different PKCs at various locations

in the cell, carrying out different functions and responses. However, regarding *in vivo* functions of PKD family members, isoform-specific data are very limited.

1.3.2.1 PKD1

PKD1, being the first identified isoform, is the most studied member and has been reported as a signal transducer in many signaling pathways. One such important function is its described involvement in intrinsic oxidative stress signaling mediated by reactive oxygen species (ROS). It was shown that stimulation of HeLa cells with H_2O_2, at concentrations that does not induce cell death due to apoptosis, results in an overexpression of PKD1 and increased nuclear factor-κB (NF-κB) activity (Storz and Toker, 2003).The latter consists of a family of transcription factors and is described to be involved in an elaborate system that allows cells to respond and adapt to environmental changes (Oeckinghaus and Ghosh, 2009). The generation of ROS was shown to recruit PKD1 to the outer mitochondrial membrane where it became activated by PKCδ dependent activation loop phosphorylation (Storz et al., 2005). Its subsequent release from the mitochondrial membrane was shown to induce the expression of manganese-dependent superoxide dismutase (MnSOD) via NF-κB activation, inducing a detoxification program of the cell. In addition, a more recent study demonstrates that PKD1 deficiency in mouse embryonic fibroblasts (MEFs) caused an increased sensitivity to ROS, leading to mitochondrial depolarization and subsequently induced apoptosis (Zhang et al., 2015). Thus PKD1 could be defined as a major regulator of ROS mediated signaling, modulating several signaling pathways in that context, thereby possibly being involved in aging processes and tumor development

1.3.2.2 PKD2

As true for PKD1 also PKD2 and 3 have been placed in a number of important signal transduction pathways. Interestingly and in contrast to PKD1 and 3, PKD2 lacks a significant nuclear accumulation upon activation (Rey et al., 2003a). Notably, only a few isoform specific studies have been published so far. One of these reports identified a gastrin mediated signaling pathway leading to the activation of PKD2 (Sturany et al., 2002). This study showed that the stimulation of AGS-B cells (human gastric cancer cell line) with gastrin leads to an immediate activation of PKD2 which was mediated by the activation of a specific G-protein coupled receptor (cholecystokinin (CCK_B)-receptor) and a subsequent PLC activation. In addition, this work also provided evidence that PKCs (most likely α, ε and η isoforms) are involved in the

activation of PKD2 after gastrin stimulation. Based on this study and the fact that gastrin has been shown to play an important role in gastrointestinal disorders and carcinogenesis (Jensen, 2002), one *in vivo* function of PKD2 might be placed in this context as well.

1.3.2.3 PKD3

The limited amount of isoform specific publications is also true for PKD3. While all PKD isoforms are mostly distributed in the cytoplasm when unstimulated, PKD3 shows in addition another distinct localization. By examining the intracellular distribution of endogenous PKD3 in unstimulated Panc-1 cells, using an immunofluorescence and western blotting approach, Rey et al. showed a very prominent nuclear localization for PKD3 (Rey et al., 2003b). In addition, a study by Chen et al., 2008, identified PKD3 downstream of Akt and ERK1/2 involved in cell growth and survival signaling in a prostate cancer cell line. Within the Leitges group at the Biotechnology center of Oslo, recent work using PKD3 deficient MEFs have identified two additional previously unknown PKD3 specific functions. First a PKCε/PKD3 specific signaling axis has been established in the context of cytokinesis (Zhang et al. unpublished). In this study a PKD3/GFP construct revealed a cleavage furrow specific localization of this construct, which was accompanied by a double/multi nucleated phenotype in deficient MEFs. In the further it could be shown that PKD3 regulates the RhoA/GTP level at the cleavage furrow during abscission. This work led to the identification of a possible PKD3 substrate, namely MP-GAP, which is supposed to regulate the RhoA/GTP levels during cytokinesis (Zanin et al., 2013). In addition to this phenotype, the characterization of PKD3 deficient MEFs also revealed a dramatic decrease of the proliferation rate when PKD3 is missing in an immortalized cell. Interestingly this phenotype was shown to be PKCε independent and the most likely cause was identified by severe alterations during microtubule nucleation and polymerization mediated by the lack of PKD3 (Zhang et al. unpublished).

1.4 Analog sensitive kinase technology

The existence of closely related kinases in eukaryotic cells defines the problem to distinguish and characterize isoform specific *in vivo* functions among these kinases. The established approach to use pharmacological inhibitors suffers from the fact that no isoform specific compounds are available since most inhibitors commercially available and described are ATP binding competitors with rather low isoform specificity. This fact represents a current bottleneck in the kinase research area. To circumvent these problems, Kevan Shokat and his

team at University of California San Francisco have developed so-called driver mutations. This particular mutation, within the ATP binding site of kinase, harbors the potential of selective inhibition (Bishop and Shokat, 1999).

In detail this approach, termed analog sensitive (AS) kinase technology, combines the use of a small molecule inhibitor with the specificity of a genetic perturbation. The approach is based on the discovery of a tyrosine kinase inhibitor (PP1) and its great affinity for kinases in the Src family. Liu et al. reported that a single residue, corresponding to Ile 338 in v-Src, in the ATP pocket was responsible for this affinity. By altering this residue, and thereby changing the ATP-pocket size, PP1 ability to inhibit could be controlled (Liu et al., 1999).

When this single residue, termed gatekeeper residue, is mutated to a residue bearing a smaller side chain (glycine or alanine), it creates a novel pocket within the ATP-binding site. This pocket is not found in the wild-type (WT) kinases, and since nearly all kinases have a bulky gatekeeper residue, the same technology application should be possible for most, if not all, kinases. The gatekeeper residue plays an important role in promoting enzymatic activity and mutation of this residue may disrupt structural features and reduce catalytic activity (Azam et al., 2008). The reduced catalytic activity is often acceptable and does not result in defects.

Mutation of the gatekeeper residue to glycine usually maximizes the difference in sensitivity between WT and mutated kinase alleles to the inhibitor, but can also cause an unaffordable reduction in activity (Lopez et al., 2014). In this case, employing an alanine gatekeeper can increase enzyme activity without fully compromising sensitivity to AS kinase inhibitors. Once the mutation is established and functional, a suitable inhibitor has to be identified. Two major classes of AS kinase inhibitors exist: staurosporine and PP1 derivatives. The most efficacious and commonly used inhibitors are 1NA-PP1 and 1NM-PP1.

The introduction of a mutation in the gatekeeper residue opens up the opportunity for isoform specific inhibition, but also direct substrate identification of protein kinases. Shokat and his colleagues have devised a chemical method for tagging the direct substrate of any protein kinase. For the labeling, a [-S] labeled ATP analog, termed N6-(benzyl)ATP, with poor substrate of wild type is used. This approach could eventually allow for the complete mapping of any kinase pathway in a cell.

1.5 Aim of the thesis

In this study, we wish to establish stable cell lines expressing various functional analog sensitive kinases of PKD isoforms 1 and 3. The idea is that these cell lines will then serve as a powerful tool aiming to increase isoform-specific data of PKD *in vivo* function. In order to establish these cell lines, vectors harboring PKD isoforms with mutated gatekeeper residue need to be generated in the first place. A Lenti-virus based expression system will be used for the exogenous expression of proteins in mammalian cells, and the analog sensitive kinases will be expressed in appropriate deficient background. We will further use established phenotypes of PKD deficient isoforms (e.g. PKD1: mitochondrial depolarization and PKD3: double/multi nucleation) to test (i) if the exogenous protein harboring the gatekeeper variant rescues the deficiency, and (ii) if a specific inhibitor (1-Na PP1) can convert the cell lines back to deficient responses.

2 Materials

Plasmids:

Entry vector pENTR^{TM}/$_{D}$-TOPO (2,6 kb), containing kanamycin resistance gene (Invitrogen, catalog number K2400-20)

and destination vector pLenti6.3/V5-Dest (7,8 kb) containing ampicillin resistance gene (Invitrogen, catalog number K5310-00).

Table 1. Restriction enzymes used

Vector	**cDNA insertion**	**Restriction Enzymes**
pENTR^{TM}/$_{D}$-TOPO	PKD1/GFP	EcoRV
		HincII and StuI
	PKD3/GFP	EcoRV and BamHI
		XbaI and NdeI
pLenti6.3/V5-Dest	PKD1/GFP	XhoI and AflII
		StuI
	PKD2/GFP	HincII
		EcoRV
		EcoRI and AflII
	PKD3/GFP	AflII
		XbaI

Table 2. Primers used for site directed mutagenesis, sequencing and genotyping.

Site directed mutagenesis		
Target	Direction	Primer sequence (5´to 3´)
PKD1 (M665A)	Forward	CCATGGAGTTTTTCCGCAACAACAAACACTCTTTCAGGCGTCTC
	Reverse	GAGACGCCTGAAAGAGTGTTTGTTGTTGCGGAAAAACTCCATGG
PKD1 (M665G)	Forward	GAGACGCCTGAAAGAGTGTTTGTTGTTGGGGAAAAACTCCATGG
	Reverse	CCATGGAGTTTTTCCCCAACAACAAACACTCTTTCAGGCGTCTC
PKD2 (M628A)	Forward	AGAAGGTATTCGTGGTGGCGGAGAAACTGCACGGGG
	Reverse	CCCCGTGCAGTTTCTCCGCCACCACGAATACCTTCT
PKD3 (M651A)	Forward	TCTCCATGGAGCTTTTCCGCCACCACGAAGACTCGTTC
	Reverse	GAACGAGTCTTCGTGGTGGCGGAAAAGCTCCATGGAGA
PKD3 (M651G)	Forward	GAACGAGTCTTCGTGGTGGGGGAAAAGCTCCATGGAGA
	Reverse	TCTCCATGGAGCTTTTCCCCCACCACGAAGACTCGTTC

Sequencing		
cDNA	Direction	Primer sequence (5´to 3´)
PKD1	Forward	TCCGGATCCAACTCACACAA
PKD2	Forward	TGATGCCCGTTATCCTCCAA
PKD3	Forward	AGGAAAACACAGAAAGACGGGA
Genotyping		
Target	Direction	Primer sequence (5´to 3´)
PKD1 (WT)	Forward	GCTTGGCATGCTTGTTTGGAGATGGG
	Reverse	GATGACAGGAGGATGCTCATGAGTGG
PKD1 (deficient)	Forward	CCTACCTTGAGCTTAGAGCAACTC
	Reverse	CCTTCTCCTCATGGAAGGGAACACC
GFP	Forward	GGCGCGCCATGGTGAGCAAGGGCGAG
	Reverse	GGCGCGCCCTTACTTGTACAGCTCTGCCA

Antibodies:

Anti-PKD/PKCμ (2052) (1:1000 dilution), anti PKD3/PKCν (2054L) (1:1000 dilution), anti-cytochrome *c* (4272) (1:500 dilution) and anti-GAPDH (2118) (1:5000 dilution) were purchased from Cell Signaling. Goat anti Rabbit HRPO (111-035-003) (1:10 000) were purchased from Jackson ImmunoResearch Lab.

3 Methods

3.1 Generation of so-called gatekeeper mutations in PKD1-3

3.1.1 Identification of gatekeeper residue

The gatekeeper residue for all the PKDs were identified by multiple alignment, using bioinformatics tools, with Src-v.

3.1.2 Site directed mutagenesis

Primers were designed using web-based QuickChange Primer Design Program available online from Agilent.

Lightning Site Directed Mutagenesis, from Agilent Technologies (cat. number 210518), was used to mutate the target vectors. This method allows for rapid, efficient, and accurate mutagenesis of small and large plasmids, and can be divided into three steps. First, a thermal cycling was performed on a sample reaction (10x reaction buffer, 10-100 ng dsDNA template ,125 ng oligonucleotide forward and reverse primer, dNTPs, QuickSolution reagent, dH_2O and QuickChange Lightning Enzyme). The primers used are listed in table 2, and the DNA templates used were entry vectors containing cDNA of PKD1/GFP and PKD3/GFP fusion protein and destination vector containing cDNA of PKD2/GFP fusion protein.

During the cycling, the primers extend without displacement and generate a mutated plasmid containing staggered nicks. Extension time must be adjusted accordingly to the plasmid size (3 minutes for plasmid containing PKD1 cDNA (6 kb in total), 5,5 minutes for plasmid containing PKD2 (11 kb in total) and 3 minutes for plasmid containing PKD3 (6 kb in total)) since this thermal cycling produces a whole plasmid and not only a fragment.

Table 3. Cycling parameters for the Quickchange Lightning Site-Directed Mutagenesis Method

Segment	Cycles	Temperature	Time
1	1	95°C	2 minutes
2	18	95°C	20 seconds
		60°C	10 seconds
		68°C	30 seconds/kb of plasmid length
3	1	68°C	5 minutes

Following temperature cycling, the product was treated with *Dpn* I. *Dpn* I is an endonuclease that is specific for methylated DNA, and will therefor digest the parental DNA template. After selection for mutation-containing DNA, the nicked vector was transformed into XL10-Gold (*E. coli*) ultra-competent cells and plated out on LB agar plates containing the appropriate antibiotic. Positive colonies were picked for isolation of plasmid DNA, using PureLink™ HiPure Plasmid Miniprep Kit from Invitrogen (cat. number K2100-03).

3.1.3 Restriction digest of plasmids after mutagenesis

To confirm the correct vector with insert, different digest reactions with restriction enzymes was performed on the isolated plasmids containing mutated DNA. Restriction enzymes cut DNA at a specific recognition nucleotide sequence, called restriction sites. Isolated plasmid DNA, along with restriction enzymes and their appropriate buffers were mixed, and dH_2O was added to a final volume of 40µl. Restriction enzymes used are listed under materials in table 1. The reaction was incubated for 1 hour at 37°C, and stopped by adding 5x loading buffer (50 nM Tris/HCl (pH 8), 25% glycerol, 5 nM ETDA, 0,2% bromophenol blue and 0,2% xylene cyanole FF). A 1,2% agarose gel (1,2% agarose in 1x TAE (40nM Tris acetate and 1mM EDTA, pH 8,2-8,4) was prepared and all samples were applied to the gel electrophoresis, to verify the cuts made by the restriction enzymes. Positive clones from the restriction digest were sent out for sequencing to confirm the mutation. Company used for sequencing was GATC Biotech, and the sequencing primers are listed in table 2.

3.2 Generation of expression vectors

Expression/destination vectors were obtained through a LR recombination following manufactures protocol (Invitrogen, cat. number: A11144). This is a universal cloning method based on the site-specific recombination properties of bacteriophage lambda, and involves two major components; the DNA recombination sequences (*att* sites) and the proteins mediating the reaction. The previously sub cloned cDNA with entry vector backbone is enclosed by two *att*L (one on each side) sites. The LR recombination reaction (100 ng Entry clone, 300 ng Destination vector, TE Buffer and LR Clonase™ II Plus Enzyme mix)) transfers the gene from a vector containing *att*L, to an *attR*-containing destination vector to create an *att*B-containing expression/destination clone and a second byproduct plasmid. The samples were incubated for 1 hour at room temperature, followed by application of Proteinase K and a 10 min incubation at 37°C. After incubation, the mixture was transformed into One Shot Stbl3 (*E. coli*) bacteria

and plated out on LB agar plates containing the appropriate antibiotic. Positive colonies were picked and plasmid DNA were isolated using PureLink™ HiPure midiprep Plasmid DNA Purification Kit from Invitrogen (cat. number K2100-05). Since the destination vector were to be used for virus production, and later expression in mouse embryonic fibroblasts (MEFs), the last step of the isolation was performed under a sterile hood. A new restriction digest was performed on the vectors, following the same protocol as described (see 3.1.3). Restriction enzymes used are listed under materials in table 1.

3.3 Establishment of gatekeeper variant expressing MEF cell lines

Due to specific safety regulations, this section was performed by the lab-engineer of the Leitges group (U. Braun)

3.3.1 Virus production using 293FT cells

The production of lentivirus was done according to the ViraPower™ HiPerform™ Lentivirial Expression System Manual from Invitrogen (cat. number A11141). All handling from this point were done in sterile environment. The 293FT cell line is a suitable host for lentivirial production. 293FT cells were cultured in complete medium following manufactures protocol. When the 293 FT cells reached a confluence of 90-95%, a mixture containing pLenti plasmid, packaging mix and lipofectamine were added to the cells through medium exchange and left over night. The packaging mix was supplied from the manufacture and contains plasmids with features required to produce the lentivirus, while the lipofectamine is a common transfection reagent. After transfection (4-5 days), the virus-containing supernatants were collected and stored at -80°C.

3.3.2 Infection of Lentiviral stock

The produced virus from step 3.3.1, containing mutated PKD1 and 3 cDNA, was added trough medium exchange to its corresponding deficient MEFs. The following day, the virus-containing medium was removed and replaced with complete medium and incubated overnight. At day 3, the medium was exchange with Blacticidin containing medium to select for stably transduced cells. Once selection was done, aliquots were made for storage.

3.4 Cell culture

All cells were incubated at 37°C in humidified 5% CO_2 and 95% air incubator (Nuaire^{TM})
The MEFs were cultured in Gibco DMEM + GlutaMAX^{TM}-I (Invitrogen) medium with 10% Gibco fetal bovine serum (Invitrogen), Gibco non-essential amino acids (Invitrogen) and pencillin-streptomycin (50 unit/ml) (Invitrogen). Phosphate buffer saline (BPS) (Invitrogen) was used for washing. When cells grww confluent they were treated with Tryps-EDTA and split onto new plates.
Cells kept in culture were: PKD1 deficient (PKD1-/-), PKD3 deficient (PKD3-/-), WT, PKD1-/- with mutated exogenous PKD1 (PKD1-M/A and M/G) and PKD3-/- with mutated exogenous PKD3 (PKD3-M/A and M/G).

3.5 Western Blot

3.5.1 Protein extraction

Cultured cells were treated with Tryps-EDTA, and cells were harvest through normal medium collection. The cells were pelleted through centrifugation at 1000 rpm for 5 min at 4°C. Whole cell extraction were obtained by resuspending the pellet in 100 µl lysis buffer (150 nM Nacl, 1% NP-40, 50 mM Tris (pH 8), 20 µg/ml Leupeptin, 20 µg/ml Aprotinin, 50 µg/ml PMSF, 0,5 mM DTT). The samples were kept on ice for 15 min, followed by 15 min centrifugation at 14000 rpm at 4°C. The protein containing supernatants were kept and the concentrations were measured using BioRad Bradford reagent (Bio-Rad, cat. number 500-0006) and Eppendorf BioPhotometer, measuring absorbance at 595 nm. A standard curve was made using bovine serum albumin (BSA), and the protein concentrations were measured accordingly. Last, 4x sample buffer (1M Tris/HCl (pH 6,8), 8% SDS, 20% glycerol, 0,1M DTT, bromophenol blue) was added to the samples, followed by 5 min boiling.

3.5.2 SDS-PAGE

The SDS polyacrylamide gel was prepared in two steps. The lower part, representing the separation gel, was composed of 8% polyacrylamide, 0,375 M Tris-Cl (pH 8,8), 0,1% SDS, 0,1% APS and 0,04% TEMED. The upper part (stacking gel) was composed of 5% polyacridamide, 0,1% SDS, 125 mM Tris-HCl (pH 6,8), 0,04% TEMED and 0,1% APS. All protein extracts were normalized, so equal amount of protein was used for electrophoresis. The samples were run at constant voltage 120 V until satisfied separation.

3.5.3 Blotting

After separation, the proteins were transferred to a Bio-Rad nitrocellulose membrane (0,45 µm) in blotting buffer (25 mM Tris, 192 mM glycine, 20% methanol) using a Hoefer apparatus for 1 hour at constant ampere (0,4 mA). The membrane was washed in 0,1% Tween-PBS (PBST) before blocked with 5% skimmed milk powder in PBST for 1 hour. After blocking, membranes were incubated with primary antibody in 5% skimmed milk PBST overnight in 4°C. The membrane was again washed in PBST, following incubation with secondary antibody for 2 hours in room temperature. Antibodies used are listed under material. Membranes were washed again before chemiluminescent detection using SuperSignal West Pico from ThermoFisher (product number 34080).

3.6 Genotyping

3.6.1 DNA extraction

30 µl of cells were collected and pelleted by centrifugation at 14000 rpm for 1 minute. The cells were resuspended in 25 µl dH_2O and boiled for 5 minutes. Proteinase K was added and the samples were incubated for 1 hour at 55°C. Last, all samples were boiled for 5 minutes.

3.6.2 PCR based genotyping

Extracted DNA, primers and Taq polymerase were mixed together and a polymerase chain reaction (PCR) was performed. This was a multi PCR, using four primers for 2 distinct bands. Primers used are listed in table 2 under materials. The PCR cycling are presented in table 4. In addition to PCR based genotyping, the same DNA extracts were tested for the existence of the GFP tag, also by PCR based approach. The same protocol and PCR cycling were used, and primers can be found in table 2. When the cycling was done, 5x loading buffer was added to each sample, and run on 1,2% agarose gel to distinguish the PCR amplicon sizes.

Table 4. PCR cycling Protocol

Segment	Cycles	Temp	Time
1	1	95°C	5 minutes
2	44	94°C	15 seconds
		62°C	30 seconds
		72°C	2 (44) 45 seconds
3	1	72°C	10 minutes

3.7 PKD1: Mitochondrial Depolarization Assay

Tetramethylrhodamine, methyl ester (TMRM) is a cell-permeant, red-orange fluorescent dye that is readily sequestered by active mitochondria.

3.7.1 Mitochondrial depolarization assay to test for rescue

WT, PKD1-/-, PKD1-M/A and PKD1-M/G cells were grown to 90% confluence on 10 cm dishes, treated with Tryps-EDTA and collected through normal medium collection. They were further pelleted by centrifugation at 200xg for 5 min. The supernatant was discarded and the pellet was washed with PBS. The pellet were further resuspended in cresol red-free medium with TMRM (0,5µg/ml) and incubated for 30 minutes at 37°C. Following incubation, the cells were washed and treated with H_2O_2 in non-serum medium for 15 minutes at 37°C. The H_2O_2 were added in two different concentrations; 25 and 50 µM. The released TMRM were washed away with PBS, and the samples were run on BD FACSCanto^{TM} II flow cytometer. The data was collect and analyzed using FlowJo software.

3.7.2 Mitochondrial depolarization assay to test for gatekeeper variant function

Following the same protocol as described above, only 2µM 1-Na PP1 was added together with the dye.

3.8 PKD3: Cell cycle regulation

Propidium iodide (PI) is a fluorescent molecule that binds DNA with little or no sequence preference, and is the most commonly used dye to quantitatively assess DNA content.

3.7.1 Cell cycle regulation to test for rescue

WT, PKD3-/-, PKD3-M/A and PKD3-M/G cells were grown to 60 % confluence on 6 cm dishes. The cells were first starved for 24 hours in 0,2% medium, followed by medium exchange to medium containing Nocodazole (NCZ) (0,1µg/ml). NCZ interfere with the polymerization of microtubules and arrest the cells in G2/M-phase in the cell cycle. After 24h NCZ treatment, the medium was replaced with normal medium for release. Five samples were collected for each genotype; control, 24 hours starvation, 24 hours treatment and 24 hours release. The samples were collected through trypsinization and normal medium collection. They were centrifuged at 200xg for 3 min at 4°C, and the pellets were resuspended with PBS. The cells were fixed using ice cold ethanol, and kept in 4°C.

3.8.2 Cell cycle regulation to test for gatekeeper variant function

Same protocol as describe over, only 2 µl and 10 µl 1-Na PP1 was added in combination with the release medium. Cells were fixed with ice cold ethanol.

3.8.3 PI staining

Samples were pelleted by centrifugation at 300 rpm for 5 min at 4°C, and the ethanol were discarded. The pellets were resuspended in 200 µl freshly prepared staining solution (0,3 mg/ml RNase and 0,04 mg/ml PI), and incubated for 45 min in the dark in room temperature. PBS was added to a final volume of 900 µl before running the samples using FACSCalibur flow cytometer. The data was collected and analyzed using FlowJo software.

4 Results

4.1 Generation of so-called gatekeeper mutations in PKD1-3

4.1.1 Site directed Mutagenesis

In order to apply specific inhibitor assays later, we had to generate responsive PKD variants in the first place. To do so we used the PCR based site directed mutagenesis approach to introduce an appropriate amino acid exchange in each PKD isoform. The initially characterized gatekeeper residue in v-Src corresponds to Ile338 and is characterized by its ability to affect PP1 inhibition. Using bioinformatics tools the following amino acid residues have been identified in PKD: PKD1: Methionine (M)665, PKD2: M628 and PKD3: M651.

Aiming to expand the ATP binding pocket all mutations were designed to introduce a less space filling amino acid (e.g. either A or G). Since there is no clear statement available about the effectiveness of one preferred amino acid exchange in this context, two individual mutagenesis were performed to introduce both mutations in PKD1 (M665A and M665G) and PKD3 (M651A and M651G) while for PKD2 only the M628A exchange was established in the given time frame. As a starting material the following plasmids, which had been generated and characterized in the group prior to this study, were used: PKD1-pENTR^{TM}/$_{D}$-TOPO containing the full length cDNA of mouse PKD1, PKD2- pLenti6.3/V5-Dest containing the full length cDNA of mouse PKD2, and PKD3- pENTR^{TM}/$_{D}$-TOPO containing the full length cDNA of mouse PKD3. In addition, each PKD had been constructed in a way to contain a green fluorescent protein (GFP) at the C-terminus. After the mutagenesis reaction, the products were transformed into ultra-competent cells and plated out on LB agar plates containing kanamycin (for entry vectors) and ampicillin (for destinastion vector) as antibiotic. After overnight incubation at 37ºC, individual colonies were picked and further cultivated, followed by a characterization with various restriction digests and subsequent sequencing.

In detail, for PKD1 EcoRV was used, which is supposed to generate four fragments in a restriction digest (2808, 1386, 1224 and 636 bp) from which 1 site originate from the plasmid backbone while 3 comes from the PKD1 cDNA. The 636 bp fragment and 1386 bp fragment represents the specific PKD1 fragment (figure 2(A) lane 1). In addition, a double digest with HincII and StuI was performed on the entry vector containing PKD1 cDNA, which is supposed to generate three fragments (4328, 1027 and 699 bp). Two of the sites originate from the PKD1 cDNA while the third originates from the plasmid backbone.

Also for the resulting PKD2 construct an EcoRV restriction digest was accomplished. In this case the expectation was again to receive four fragments with the predicted sizes of 7638, 1779,

1293 and 391 bp. All four EcoRV sites are located in the vector backbone, which makes the biggest fragment, 7638 bp, the specific fragment containing the PKD2 (figure 2(B) lane 2). In addition, another restriction digest was accomplished using HincII restriction enzyme on the destination vector containing PKD2 cDNA. This reaction produces three fragment (5828, 4577 and 696 bp), from which all three sites are located in the vector backbone, producing a 5828 bp fragment specific for the PKD2 cDNA insertion (figure 2(B), lane 1). A third digest was performed for the destination vector containing PKD2 cDNA using two enzymes; EcoRI and AflII. This reaction also produces three fragments (5223, 3656 and 2222 bp), from which one site is located in the PKD2 cDNA, making the 5223 bp fragment specific for PKD2 cDNA.

In case of the PKD3 construct, a double digest using EcoRV and BamHI was performed. This restriction digest was supposed to produce two fragments (5117 and 873 bp), from which one site is located in the PKD3 cDNA, making both fragments specific for the PKD3 cDNA insertion (figure 2(C), lane 1). Another double digest was performed on the vector using XbaI and NdeI, producing three fragments (3879, 1429 and 629 bp). All three sites are located in the PKD3 cDNA, making all produced fragments specific for PKD3 cDNA content (figure 2(C). lane 2).

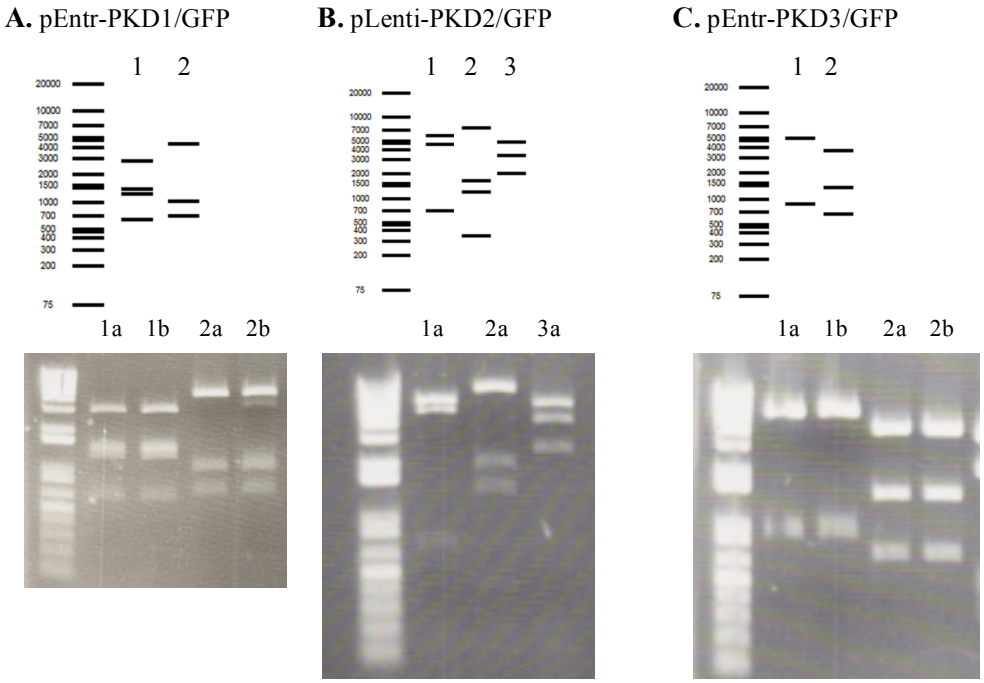

Figure 2. Plasmid characterization using restriction digest. A – Restriction digest with (1) EcoRV and (2) HincII and StuI on pEntr/D-TOPO containing PKD1-GFP M665A(a) and M665G(b). B - Restriction digest with (1) HincII, (2) EcoRV and (3) EcoRI and AflII on pLenti6.3/V5-Dest with PKD2-GFP M628A (a) insertion. C – Restriction digest with (1) EcoRV and BamHI on pEntr/D-TOPO containing PKD3-GFP M651A(a) and M651G(b) insertion.

Taken together all restriction digests revealed the content of the appropriate PKD cDNA by the correct pattern (figure 2). In order to verify the individual inserted mutations several clones for each mutation with the correct pattern were chosen and send out for sequencing (service used: GATC Biotech). According to the sequencing results, one clone of each mutation was selected for further processing (PKD1-M/A; -M/G, PKD2-M/A, PKD3-M/A; -M/G). An alignment of the corresponding WT versus mutant sequence is shown in figure 3 indicating for each mutation the predicted and observed nucleotide exchange.

```
pEntr_PKD1-GFP(M/A)   281    TTGTTGTTGCGGAAAAA
                             ||||||||   |||||||
cDNA_PKD1             2235   ttgttgttatggaaaaa
                             ||||||||   |||||||
pEntr_PKD1-GFP(M/G)   281    TTGTTGTTGGGGAAAAA

pEntr_PKD2-GFP(M/A)   320    TCGTGGTGGCGGAGAAA
                             ||||||||   |||||||
cDNA_PKD2             2433   tcgtggtgatggagaaa

pEntr_PKD3-GFP(M/A)   145    TCGTGGTGGCGGAAAAG
                             ||||||||   |||||||
cDNA_PKD3             2708   tcgtggtgatggaaaag
                             ||||||||   |||||||
pEntr_PKD3-GFP(M/G)   145    TCGTGGTGGGGGAAAAG
```

Figure 3. Sequencing result for mutated clones. Sequencing results aligned with corresponding WT sequence for each isoform. Sequencing data are in capital letters and the mutations are highlighted. The position of the first residue is indicated before the residue.

4.1.2 Generation of Lenti vectors

For the exogenous expression of proteins in mammalian cells, we chose a Lenti-virus based expression system, in combination with the gateway system. The prerequisite for this approach is the establishment of so-called *destination vectors,* which later are used for virus production under controlled conditions. Viruses are then later used for infection and subsequent protein expression in the appropriate MEF lines. Thus individual cDNAs of PKD1 and 3, harboring the corresponding gatekeeper mutation, were sub-cloned into a specific destination vector backbone containing all requested properties (in our case: pLenti6.3/V5-Dest). With regard to PKD2, the mutagenesis had already been accomplished on such a vector backbone.

For the individual sub-cloning of PKD1 and 3 corresponding pEntr/D-TOPO vectors harboring each cDNA together with the pLenti6.3/V5-Dest plasmid were applied to a LR recombination reaction. Based on this specific reaction, cDNAs from entry vectors will be recombined into the target destination vector backbone (see section 3.2 for a detailed description). After incubation, each LR reaction was then transformed into ultra-competent bacteria, and plated out on ampicillin containing LB agar plates. Through antibiotic selection, only colonies with a successful recombination grew. Several colonies were then picked and cultured overnight.

Subsequent plasmid DNA was prepared and a further characterization of the containing plasmids by specific restriction digests was carried out.

In detail, for PKD1 a double digest using XhoI and AflII was performed, which is supposed to generate three fragments (5859, 3656 and 1727 bp) from which all sites are located in the vector backbone, making the 5859 bp fragment specific for an insert. In addition, the destination vector with PKD1 cDNA insert was treated with StuI, generating three fragments (6004, 4024 and 1214 bp), from which one site is in the PKD1 cDNA. The 4024 bp fragment is specific for PKD1.

Regarding destination vector containing PKD3 cDNA a restriction digest using AflII, which was supposed to produce two fragments (7486 and 3656 bp). One of the two sites are located in the PKD3 cDNA, making the 3656 bp confirm the PKD3 cDNA insertion. An additional digest reaction was performed on this vector using XbaI. XbaI produces four fragments (7606, 2111, 1214 and 247 bp), from which two sites are located in the PKD3 cDNA, producing two specific fragments from the PKD3 cDNA; 2111 and 1214 bp.

Taken together, all mutated cDNAs were successfully transferred into pLenti6.3/V5-Dest vectors and verified.

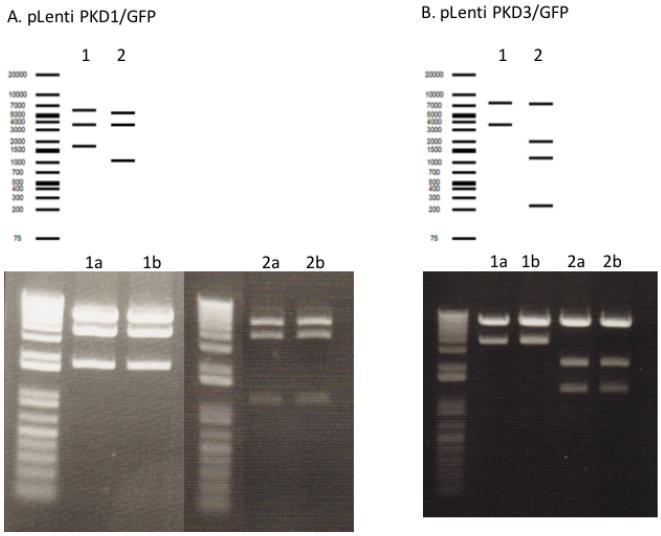

Figure 4. Restriction digest on destination vector containing PKD1/GFP and PKD3/GFP cDNA. A – Restriction digest with XhoI and AflII(1) and StuI (2) performed on pLenti6.3/V5-Dest PKD1-M/A (a) and M/G (b). B – Restriction digest with AflII (1) and XbaI (2) performed on pLenti6.3/V5-Dest PKD3-M/A (a) and M/G (b).

4.2 Establishment of gatekeeper variant expressing MEF cell lines

Next, Lenti-viruses carrying the modified cDNAs of each PKD needed to be produced. Since all steps included in this procedure are under specific safety regulation, the whole protocol was performed in collaboration and supervision of the lab-engineer of the Leitges group (U. Braun). Once these viruses were produced, we were able to proceed with the establishment of MEFs lines expressing PKD variants. Therefore, the establishment of the expressing cell lines can be divided into two steps; first being the virus production and second the virus infection of MEFs.

4.2.1 Virus production using 293FT cells

293FT cells (representing an optimized cell type, see section 3.3.1) were used for this approach. With the help of a provided packaging mix destinations vectors for PKD1 and PKD3 gatekeeper mutations were transfected. The usual protocol includes an overnight incubation after transfection followed by a further two day incubation. The production of virus related proteins causes the cells to fuse resulting in large multinucleated cells, which can be taken as a positive control by visual examination for the success of the transfection. Supernatants are supposed to contain the produced virus particles and were harvested and stored after incubation. Since a PKD2 deficient MEF line does not exist we relinquish to proceed with the PKD2 construct at this end. But for PKD1 and 3 we carried on to produce Lent-virus stocks, which were used in the following.

4.2.2 Virus infection into MEF cell lines

In total four different viruses were used for the further work (PKD1-M/A, PKD1-M/G, PKD3-M/A and PKD3-M/G). Applied MEFs were either PKD1 or PKD3 deficient. The reason behind is based on the fact that in the first place the introduction of each gatekeeper construct is supposed to rescue the corresponding PKD phenotype (e.g. PKD1 – mitochondrial depolarization defect; PKD3 – microtubule associated cell cycle delay), thereby providing a verification of the functionality of the introduced constructs.

Following the strict regime indicated in the manufacture's protocol, individual deficient MEFs were infected with the corresponding virus particles and selected for blasticidin resistance, in order to establish stable expressing cell lines. For all viruses we have been able to establish stable cell lines but with different efficiency. It appears that the general ability to infect and establish $PKD3^{-/-}$ MEFs expressing the gatekeeper construct was significantly reduced when compared to the approaches using $PKD1^{-/-}$ MEFs. This could in principle be recognized by the

fact that fewer colonies after selection were observed, thus as a consequence the establishment of stable cell lines took significantly longer.

Nevertheless, for both attempts a first rough inspection revealed that the introduced gatekeeper constructs appeared to rescue the original observed phenotype. In detail, PKD1 deficient MEFs transfected with both gatekeeper variants, established as stable cell lines, survived an overnight starvation without indicating a vast increase of apoptotic cells, inspected by visual examination, which was taken as a first indication of a functional rescue.

With respect to PKD3 the introduced gatekeeper constructs were able to rescue the slow down of the proliferation rate, when compared to WT MEFs, and the increased number of double/multi nucleated cells during standard cell culture condition disappeared. Thus also for PKD3 both gatekeeper constructs appeared to functionally rescue the deficient phenotype.

4.2.3 Western blot analysis in order to verify exogenous protein expression

To ensure that exogenously integrated expression constructs are expressed in the target cell a standard procedure for verifications is the western blot analysis. Thus each established MEF line was applied to such an analysis in the first place. In general proteins were extracted using a whole cell extraction protocol followed by a separation by SDS-PAGE. The SDS-PAGE was followed by a transfer (blotting) onto a nitro-cellulose membrane, which then was used for the antibody incubation. Isoform-specific antibodies for PKD1 and 3 were applied in the detection and by the predicted protein sizes for PKDs it was expected that endogenous PKD1 and 3 could be detected at around 105 kDa while both PKD/GFP fusion protein should increase their size of about 25 kDa (e.g. 130 kDa) due to their C terminal GFP tag.

With regard to PKD1 the first western blot analysis revealed surprisingly a PKD1 specific band at the size of the endogenous protein (figure 5, lane “PKD1-M/A”), while the PKD1 deficient extract verified the antibody specificity (figure 5, lane “PKD1$^{-/-}$). To ensure that the applied MEF line used for the virus infection represented a PKD1 deficient genotype we performed a PCR based genotyping for the predicted PKD1$^{-/-}$; PKD1-GFP (M/A) cell line in comparison with wild type material. As indicated in figure 6(A) the PKD1 specific genotyping revealed that both predicted PKD1 deficient lines in fact showed the deficient genotype while the WT control only showed the corresponding WT band.

Thus since the genotypes appeared to be correct we tested for the existence of the GFP tag also by a PCR based approach (figure 6(B)). Indeed, this analysis revealed the lack of a GFP signal in the PKD1-M/A cell line while a PKD3-M/A cell line showed the expected signal, see figure 6(B).

We then went back to the parental plasmid (pEntr/$_D$-TOPO PKD1/GFP), which was used for the original mutagenesis. In fact, it turned out that this construct didn't contain a GFP tag as it should, analyzed by a specific restriction digest with EcoRV, which should generate a specific fragment of 1386 bp but the size was reduced due to missing GFP sequence (data not shown). Thus we concluded that a mix up of constructs happened at the very beginning of this part of the project and since this effected the M/G as well as the M/A mutagenesis for PKD1, we initiated a new mutagenesis on a pEntr/D-TOPO vector containing a PKD1/GFP cDNA which was verified by several restriction digest before the mutagenesis. Restriction digest earlier shown are all based on these newly established constructs.

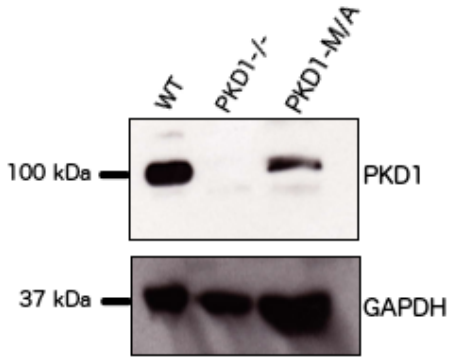

Figure 5. Western blot analysis showing expression of exogenous protein. Whole cell extracts from wild-type, PKD1-/- and PKD1-M/A cell lines. The applied antibodies for detection are indicated next to the graph. GAPDH was used as loading control.

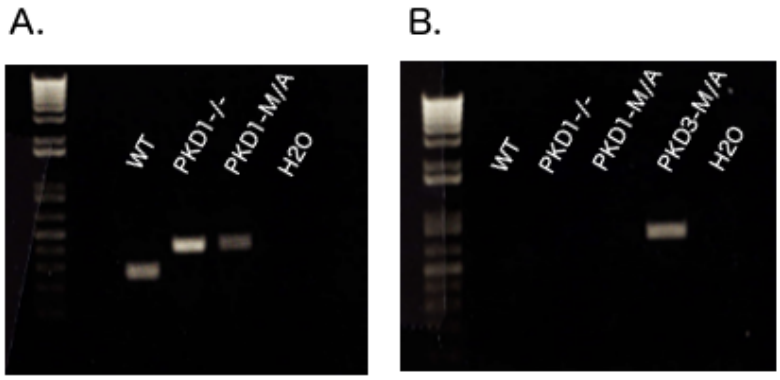

Figure 6. Genotyping of cell lines. A – PCR based genotype on extracted DNA from WT, PKD1-/- and PKD1-M/A. PKD1-WT allele primers produces a 269 bp fragment while the PKD1 knockout primers produce a 405 bp fragment. B – PCR based approach using GFP detecting primers on extracted DNA from WT, PKD1-/-, PKD1-M/A and PKD3-M/A. GFP primers produce a 737 bp fragment.

Newly established PKD1-M/A and -M/G MEFs were then also applied to a western blot analysis. As indicated in figure 7(A), this time we were able to detect the predicted PKD1/GFP fusion protein, but in addition we also detected a recombinant protein band at the same size as the endogenous PKD1 protein for both established cell lines. Again a PCR based genotype analysis was performed and confirmed the PKD1 deficient background of the infected MEFs (figure 7(B)). Based on the assumption that the PKD1/GFP fusion protein might represent a rather unstable protein and gets cleaved into its PKD1 and GFP parts we intended to perform a GFP specific western blot, expecting to identify a 27 kDa band in addition to the 150kDa PKD1/GFP fusion protein. Unfortunately, the GFP specific antibody used produced a massive background which makes it difficult to interpret the obtained results. Thus an optimization of the procedure is needed but wasn't executed due to time constrains. Nevertheless, we took our results from figure 7(A) as strong evidence that a PKD1 specific gatekeeper protein is expressed at same levels as the endogenous PKD1 protein in WT MEFs, suitable enough for proceeding with the functional analysis.

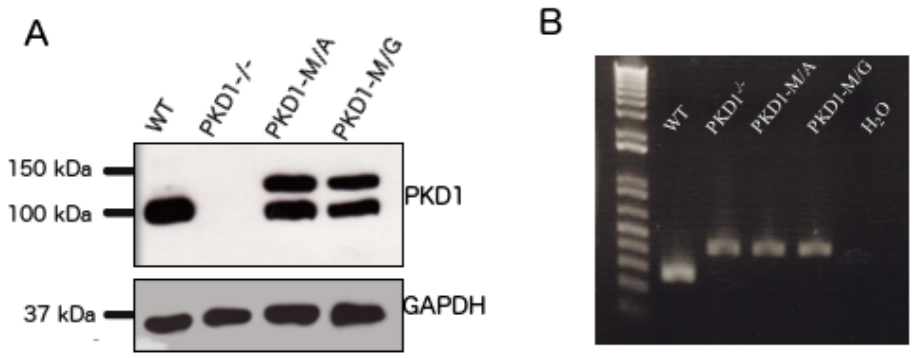

Figure 7. Western blot analysis and PCR based genotyping of PKD1 cell lines. A – Western blot analysis using whole cell extracts from WT, PKD1$^{-/-}$, PKD1-M/A and PKD1-M/G cell lines. The applied antibodies for detection are indicated on the right side of the figure. GAPDH was used as loading control. B – PCR based genotyping on DNA extracted from WT, PKD1-/-, PKD1-M/A and PKD1-MG. PKD1-WT allele primers produces a 269 bp fragment while the PKD1 knockout primers produce a 405 bp fragment.

With regard to PKD3 we succeeded to establish for both gatekeeper mutations stable cell lines. But the western blot analysis revealed that the expression of the gatekeeper was extremely low. In particular, the expression of the PKD3-M/A construct was less than 5% of the endogenous PKD3 levels in the wild type (data not shown) so that we decided to not proceed with this cell line. Also the expression levels of the PKD3-M/G appeared to be low when compared to wild type levels of PKD3 (see figure 8). Nevertheless, since we observed a functional rescue for the

PKD3 deficient phenotype (see 4.2.2) we decided to use this established MEF line for the further characterization.

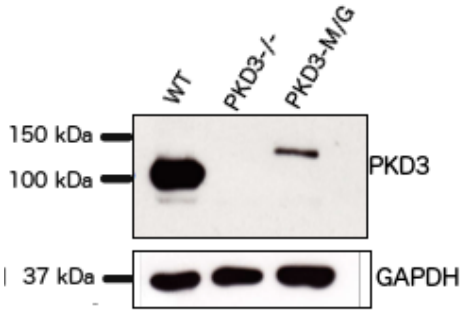

Figure 8. Western blot analysis showing expression of exogenous protein. Whole cell extracts from wild-type, PKD3$^{-/-}$ and PKD3-M/G cell lines were analyzed. The applied antibodies for detection are indicated next to the graph. GAPDH antibody was used as loading control.

4.3 PKD1: Mitochondrial Depolarization Assay

PKD1$^{-/-}$ MEFs have been shown to be sensitive to ROS mediated induced apoptosis caused by mitochondrial depolarization (Zhang et al., 2015). As a result, PKD1$^{-/-}$ MEFs show an increased number of apoptotic cells when overgrow or starved, which can be estimated by visual inspection. As indicated above, starved PKD1$^{-/-}$ cells with introduced PKD1-M/A and M/G constructs led to the conversion of this phenotype back to wild type. In the further characterization we intended to show (i) that this observation relates to the recovery of the mitochondrial depolarization mechanism and (ii) that the gatekeeper constructs are responsive to a specific inhibitor thereby converting again the rescued phenotype back to the deficiency.

Mitochondrial depolarization can be induced by H_2O_2 applied to cells at certain concentrations and analyzed by the fluorescent means (see section 3.7). As indicated in figure 9, 25µM H_2O_2 is not able to depolarize the mitochondrial membrane in wild type MEFs, but 50µM H_2O_2 does as indicated by the left shifted peak, indicating the loss of fluorescence dye from the mitochondria due to depolarization. In contrast PKD1 deficient MEFs respond already to 25µM H_2O_2 with a mitochondrial depolarization (figure 9) as described in Zhang et al., 2015. Interestingly both gatekeeper constructs (M/A and M/G) were able to rescue the original phenotype and mediate unresponsiveness to 25µM H_2O_2 treatment while the 50µM H_2O_2 response was similar to the wild type performance (figure 9).

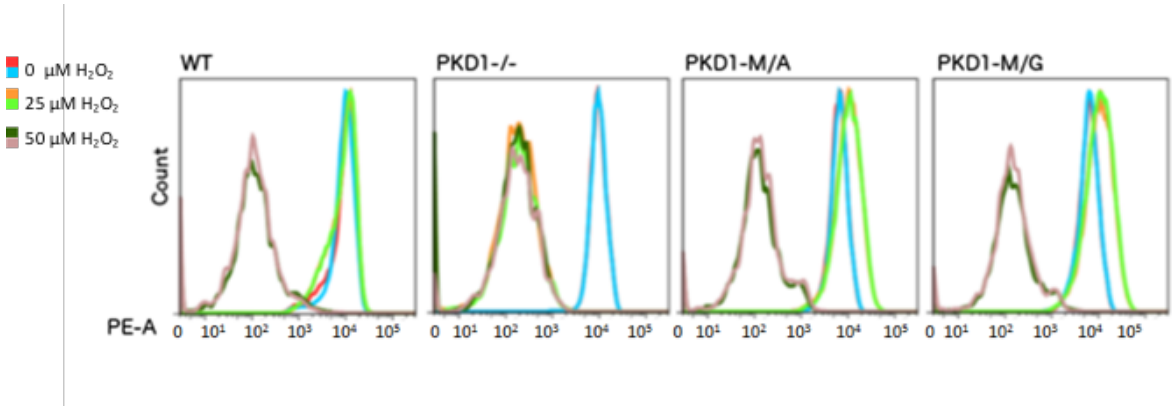

Figure 9. Mitochondrial depolarization in MEFs of various genotypes. Histograms of depolarization using TMRM, were depolarization is indicated by the loss of the dye. Blue and red lines indicate cells treated with 0 µM H_2O_2, orange and light green indicate 25 µM H_2O_2 treatment, while dark green and brown indicate 50 µM H_2O_2. Genotypes tested are indicated on the top of each histogram.

In addition, when a specific inhibitor (1-Na PP1) was applied in these assays, acting specifically on the gatekeeper constructs, both variants (M/A and M/G) showed again a depolarization response already after 25µM H_2O_2 treatment (figure 10). When comparing the mitochondrial depolarization for the PKD1 gatekeeper variant cell lines with the WT treated with 50 or PKD1$^{-/-}$ treated with 25µM H_2O_2 (figure 9) the shift appeared less pronounced. Interestingly there was no difference detectable between the M/A versus the M/G mutation, which has been described earlier.

Thus it can be stated that both gatekeeper mutations for PKD1 are able to rescue the original described phenotype of the PKD1 deficiency in MEFs and that they respond to the application of a specific inhibitor which makes these newly established cell lines suitable for future attempts.

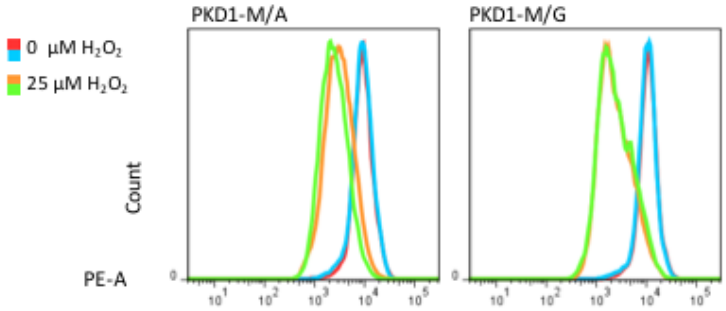

Figure 10. Mitochondrial depolarization in gatekeeper variants with 2µM Na-PP1. Histograms of depolarization using TMRM, were depolarization is indicated by the loss of the dye. Blue and red indicate 0 µM H_2O_2 treatment, while green and orange indicate 25 µM H_2O_2. Genotypes tested are indicated on top of each histogram.

4.4 PKD3: Cell cycle regulation

Ongoing studies in the Leitges group have identified a robust and diverse participation of PKD3 on the regulation of the cell cycle after immortalization on different levels. The analysis of $PKD3^{-/-}$ MEFs revealed a higher percentage of double/multi nucleated cells which has been linked to failures during cytokinesis (not published) and a drastic reduction in the proliferation rate which became associated with malfunctions during microtubule nucleation and dynamics (Zhang et al., 2016 in press).

Due to the earlier indicated problem during the establishment of PKD3 deficient MEFs expressing PKD3 gatekeeper constructs at reasonable levels we only applied one stable expressing $PKD3^{-/-}$;PKD3-M/G cell line. A rough first analysis revealed that the increased numbers of double/multi nucleated cells decreased to wild type levels and that the proliferation performance during normal cell culture was indistinguishable from the wild type. Thus the first characterization implied that the introduce PKD3-M/G gatekeeper construct is functional.

For the further characterization we applied a propidium iodide (PI) staining followed by a FACS analysis in order to analyze the cell cycle performance of the PKD3 gatekeeper construct. In general PI binds to DNA and can be used to monitor the cell cycle performance (details see section 3.8).

As indicated in figure 11 wild type cells under normal growth conditions show the majority of cells are diploid (G1/G0-phase). Starvation led to an increase of the diploid population and a reduction of the tetraploid population, while nocodazole (NCZ) treatment synchronizes cells at M-phase (tetraploid peak, see figure 11). Subsequent removal of NCZ and release after 24 h reverses the cells to original performance. In contrast, PKD3 deficient MEFs already indicate by the increased tetraploid peak in the PI staining a problem during the cell cycle. Starvation did not work as efficient as in the wild type but still decreases the tetraploid peak (figure 11) while NCZ again synchronizes cells at the M-phase. At this point it is worthwhile to mention that NCZ treatment also causes an increase of multiploid cells in the PKD3 deficient background. The following NCZ release clearly indicate a severe problem of PKD3-/- MEFs during the exit of the mitosis which has been linked to malfunction in microtubule dynamics (Zhang et al., 2016 in press).

Interestingly the introduction of a PKD3 specific gatekeeper construct converts the PKD3 deficient behavior back to a wild type performance, e.g. small tetraploid peak during normal cell growth, same response to starvation and NZC synchronization and in time release after treatment. Thus this analysis confirms the ability of the gatekeeper construct to rescue the PKD3 deficient phenotype.

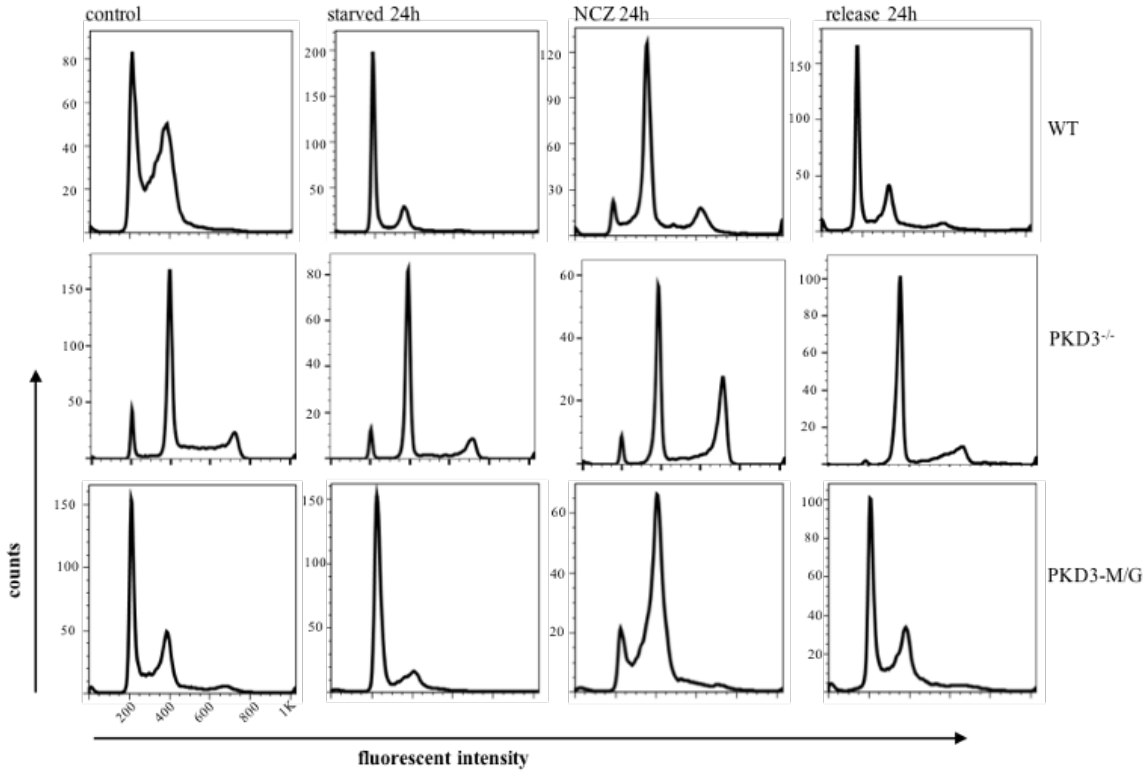

Figure 11. Propidium iodide (PI) based analysis of the cell cycle of WT, PKD3$^{-/-}$ and PKD3-M/G. Four samples collected for each genotype, and are indicated at the top of the histograms. Genotypes tested are indicated on the right side of the histograms.

Next we proceeded with a specific inhibitor experiment in order to verify the effectiveness of the gatekeeper construct. Since we had observed a high amount of dead cells in NCZ treated cells expressing the PKD3-M/G construct for unknown reasons (data not shown) we excluded this step in the following. Thus the 1-Na PP1 analog was added right after starvation into the release medium (at concentrations 2 and 10 μM) and cells were analyzed 24 h after release. In case the inhibition worked, cells incubated with the inhibitor should mimic the observed PKD3 deficient phenotype, e.g. the tetraploid peak after starvation and 24 h release should be significantly increased. No 24 h release sample with 10 μM PP1 analog were collected for the PKD3$^{-/-}$ cell lines.

As shown in figure 12, wild type MEFs behave as predicted: starvation causes the depletion of the small tetraploid peak whereas cells after release recover within 24 h. Noteworthy at this point is that the application of the inhibitor seemed to have no impact at all on wild type cells. Unfortunately, the PKD3$^{-/-}$ cells in this experiment appeared to not respond to the starvation and therefore do not serve as a proper control for this experiment. Nevertheless, PKD3$^{-/-}$ MEFs expressing a PKD3-M/G gatekeeper construct showed in the untreated control a conversion

into wild type by the pronounced diploid peak and a significant response to starvation (figure 12). The application of the inhibitor leads to a significant increase of the tetraploid peak, more so for the higher concentration, which could be taken as evidence for its functionality. To what relation this could be interpreted as a complete response is not clear yet and need further experimental evaluation.

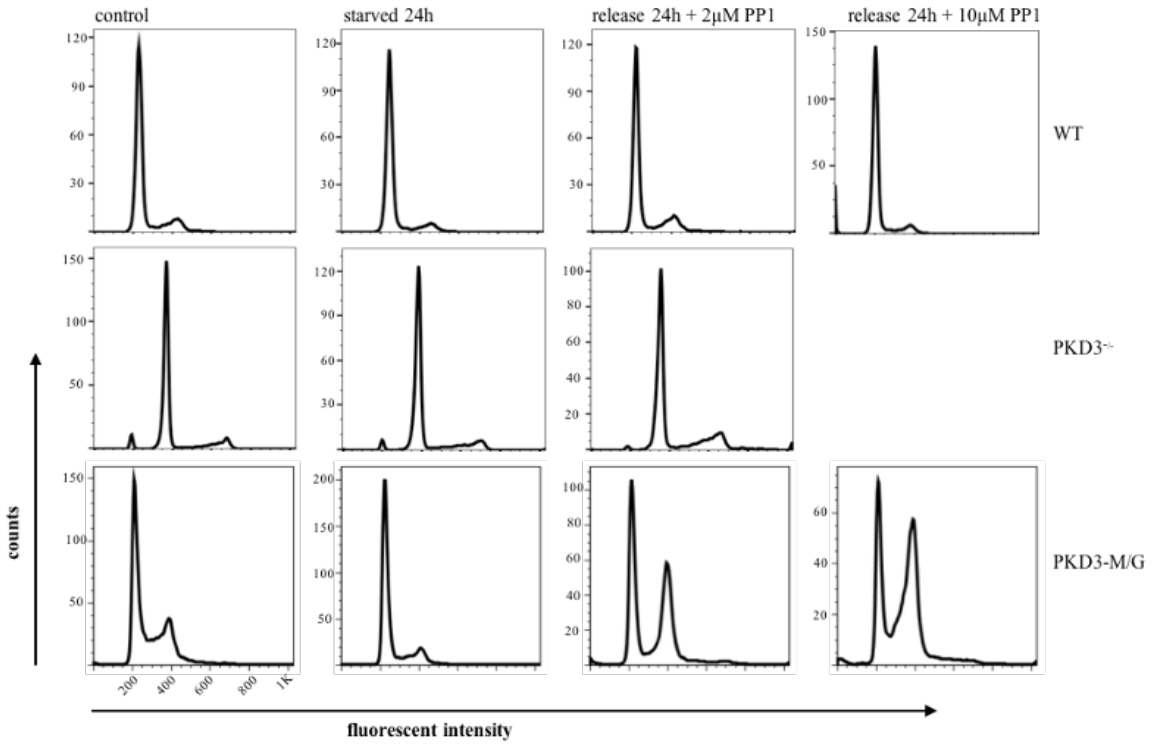

Figure 12. Propidium iodide (PI) based analysis of the cell cycle of WT, PKD3$^{-/-}$ and PKD3-M/G with respnce to 1-Na PP1. Control, 24 hours starvation and 24 release with inhibitor samples for WT, PKD3-/- and PKD3-M/G collected, stained with PI and analyzed using FACSCalibur flow cytometer.

5 Discussion

5.1 Establishing stable cell lines expressing various gatekeeper constructs

Although virus containing the M/A and M/G gatekeeper variants of PKD1 and PKD3 were produced and subsequent stable cell lines were successfully established, the ability to infect and establish PKD3$^{-/-}$ MEFs expressing the gatekeeper mutants was substantially reduced when compared to the same approach using PKD1$^{-/-}$ MEFs. The establishment of the former took longer time, as a consequence of significantly fewer colonies after selection. The observed amount of survived colonies after selection can be taken as information about how efficient the individual infection was. In general, lentivirus targets dividing cells with a higher efficiency then non-dividing (Kurian et al., 2000). Thus since PKD3 deficient MEFs were shown to have a severely reduced proliferation rate (Zhang et al., 2016 in press), a less successful infection rate could be explained accordingly. Since the mutagenesis and generation of the lentiviruses followed a well-established protocol in the lab, these factors were not questioned in the first place.

5.2 Western blot analysis

During the expression analysis of the exogenous proteins for the newly established cell lines, we came across a surprising discovery. Both PKD1 gatekeeper variants revealed a PKD1 specific band at the size of the endogenous protein (105 kDa) in addition to the exogenous PKD1/GFP fusion protein (130 kDa). Figure 7 verifies the specificity of the applied antibody due to no unspecific signals in PKD1$^{-/-}$ extracts. Since both PKD1 gatekeeper variants were infected into PKD1$^{-/-}$ MEFs, there shouldn't be any endogenous PKD1 in these cell lines. Thus one possibility for the existence of such an endogenous protein could be that the assumed PKD1$^{-/-}$ background was instead a WT or PKD3$^{-/-}$ background, which might have resulted from a mix up when MEFs were infected. Fortunately, a PCR genotyping of the established cell lines proved that they were indeed PKD1$^{-/-}$, and therefore also excluded any cross contamination prior and post infection. Ruling out any endogenous protein sources, the observed additional signal must have originated from the exogenous PKD1/GFP protein. Since the observed size mimics that of PKD1 without a GFP tail, the signal could represent a cleavage product between PKD1 and GFP. For this theory to prove right, a western blot using a GFP antibody should reveal two signals; one representing the PKD1/GFP fusion (105 kDa) and the other only GFP (25 kDa). Unfortunately, the GFP antibody used showed a very high background in the western blot analysis (data not shown) thus a severe optimization of the blotting and detection

conditions are needed, but so far no successful GFP blot was produced in the given time frame. We can therefore only speculate that the GFP tail is cleaved off, either in the cells or during the extraction procedure, resulting in a 105 kDa PKD1 signal. Nevertheless, the PKD1 gatekeeper variant cell lines showed a good expression of the exogenous protein when compared to that of WT.

Regarding the newly established PKD3 gatekeeper variant MEFs, expression of the exogenous protein was rather low when compared to that of the WT control. As earlier mentioned, PKD3$^{-/-}$ cells have a slow proliferation, which will affect the virus infection. From the observation after infection, we know that only a few cells do get infected (see section 5.1).

The overall weak expression obtained from the exogenous protein suggests that the infection rate per cell is also too low. Although several viruses target the same cell, only a few succeed with the integration into the target genome. In order to access the target genome, the virus need to traverse the nuclear envelope, which selectively controls the transport of molecules between the nucleus and the cytoplasm. However, the nuclear envelope is removed for a brief period during mitosis, which allows the viral genome to enter (Durand and Cimarelli, 2011). Unfortunately, this provides an obstacle for infection of non-divide cells and also slow proliferating cells, leading to few successful infections and low viral copy number per cell. One factor that influences the quantity of the infection is the titer of the individual virus stock. In our case, this is not measured and it is therefore not known if we applied a high or low titer. However, if a virus titer is too high, it is expected to see many dead cells, which was not the case. In addition, the expression of exogenous PKD1 gatekeeper construct is significantly higher, and since the same protocol was followed for both the most likely reason is that the titer was too low for the PKD3$^{-/-}$ approach, subsequently resulting in low expressing cell lines. To increase the expression level for PKD3$^{-/-}$ cells expressing mutated PKD3 constructs, the titer should be evaluated first and subsequently optimized for this approach. It is worth noting that the lentiviral construct can integrate into a chromosomal region that silences the CMW promotor, subsequently resulting in no gene expression, thereby losing expression. We did in fact observe a strong GFP signal from the PKD3-M/G cell line early after the infection, which became weaker later on. This might suggest that some of the viral genome had integrated in regions that silences the expression.

When dealing with a slow proliferation cell line it appears therefore crucial to optimize every condition, from the quality of the expression vector, the health of the 293FT cells all the way down to the concentration of the antibiotic used, to be able to have the most success in expression.

For this particular cell line, the elevated tetraploid population arose after immortalization and primary PKD3-/- cells do have good proliferation. In theory, this would increase the infection efficiency and expression. Unfortunately, when primary cells go through senescence, many cells die regardless, and the high expressing cells might be gone.
Regardless of the low expression, the introduced PKD3 gatekeeper construct were able to rescue the slow proliferation and it was therefore decided to proceed with this low expressing cell line.

5.3 Functional assays

5.3.1 PKD1; Mitochondrial depolarization assay

One major concern when dealing with the analog sensitive kinase technology is whether the alteration of the ATP pocket will affect the enzymatic activity of the targeted kinase. If the kinase harboring the gatekeeper mutation is about to lose its activity, the technology couldn't be applied. We already know that the PKD1 constructs are well expressed, but it is necessary with a functional assay to establish the *in vivo* activity of the exogenous protein. Aiming to determine the activity for the PKD1 gatekeeper variants, mitochondrial depolarization upon induced oxidative stress was monitored. It has been established before that PKD1 is associated with ROS-mediated cellular responses regarding mitochondria induced cell death (Zhang et al., 2015). Accordingly, the lack of PKD1 result in an increased sensitivity of ROS-mediated responses and subsequent depolarization of the mitochondria. To induce stress, H_2O_2 was applied at a given time and a certain concentration. As shown by Zhang et al., 2015, treatment with 25μM H_2O_2 is the most critical one, since WT cells can withstand this concentration while $PKD1^{-/-}$ MEFs respond with a mitochondrial depolarization. Indeed, no depolarization was observed after 25 μM treatment of H_2O_2 for the two PKD1 gatekeeper variants (figure 9), providing evidence that the enzymatic activity of the exogenously expressed PKD1 protein is able to rescue the deficient phenotype. Due to the induced cell death and subsequent cell count loss, the 25μM treated PKD1-/- and 50μM treated samples of all cell lines gave a reduced peak of cell count. This is most likely caused by the extended time used on the experiment from beginning to endpoint. Even though WT cells can withstand 25 μM H_2O_2, this is still a fairly high concentration, and 50 μM H_2O_2 is an even more severe high amount of this cell damaging agent. The assay is designed for the given time frame (15 min treatment), and an extension of the time used for the whole experiment, will result in a prolonged ROS mediated response. A

consequent of such is an increase in cell death that will subsequently affect the cell count, resulting in a wider and decreased peak then what is expected.

Furthermore, when both PKD1 gatekeeper variants were incubated with 1-Na-PP1 inhibitor they failed to initiate the appropriate responses when treated with 25μM H_2O_2. This is indicated by the left shift in figure 10. The reason for this observation being that the PP1 analog successfully inhibits both variants, resulting in a response which mimics the PKD1 deficient phenotype, e.g. mitochondrial depolarization at 25 μM. When compared to mitochondrial depolarization of WT or PKD1$^{-/-}$ (figure 9), the shift was not as pronounced. This is most likely due to a suboptimal application of the inhibitor. With regard to the mutations (M/A versus M/G), no significant differences among the two were observed in their response to 1-Na-PP1. Based on the literature, the exchange to glycine, creating the biggest pocket in the ATP binding site, is most critical with respect to any loss of enzymatic activity of a given kinase. The exchange to alanine however, would if anything be expected to be less sensitive to the PP1 analog compared to that of glycine. Neither loss of the *in vivo* activity for the M/G exchange (indicated by the rescue) nor a decreased affinity of the PP1 analog for the M/A exchange was observed. We have therefore successfully established both PKD1 gatekeeper variant cell lines. Aiming to improve this assay, a higher concentration and also a longer incubation of the inhibitor should be applied to optimize the depolarization. Unfortunately, the effect of the inhibitor towards WT cells were not tested, and we cannot fully conclude the specificity of the inhibitor towards the analog sensitive kinase before this is done.

5.3.2 PKD3: Cell cycle regulation

Although weakly expressed, the exogenous PKD3-M/G was able to perfectly rescue the PKD3 deficient cells (figure 11), which was expected based on previous cell behavior observations. In addition, figure 11 shows that the PKD3$^{-/-}$ cells applied in this experiment (which also served as parental cell line for the lentivirus infection) contain a dominant tetraploid cell population. Thus this cell stock shows a severely reduced proliferation rate, even more than previously recorded (Zhang et al., 2016 in press). Remarkable even the weak expression of the PKD3 construct is able to fully restore the wild type performance in these cells after infection and establishment as a stable cell line. As reported, the established double/multi nucleated phenotype of PKD3$^{-/-}$ cells is a result of different malfunctions causing an arrest of the cells in M phase of the cell cycle. As to why this small amount of the PKD3 gatekeeper construct is able to rescue the PKD3$^{-/-}$ phenotype could possibly be due to increased activity, or simply because only a few active PKD3 molecules are required to restore normal cell cycle. However,

the severely reduced proliferation rate observed in this particular PKD3$^{-/-}$ stock resulted in nearly no response to the applied starvation, and subsequent NCZ synchronization following an established regime, thus could not serve as a proper, ultimate control for this experiment, unfortunately. Remarkable again is the fact that this stock served as parental cell line for the PKD3-M/G infection which completely reverts the cell cycle performance to wild type (figure 11). In addition, a closer look revealed that the tetraploid population observed for WT is smaller than average (figure 11). Most likely this is due to contact inhibition as a result of a too confluent dish as it was used for this experiment. In order to improve this assay, a PKD3$^{-/-}$ cell line with a less established tetraploid population should be used, which either can be achieved by an extended period in the cell culture (which has been shown to increase the diploid population to a certain content) or the usage of another cell stock. In addition, the confluency of the cell used in the assay should be kept around 80-90%.

Finally, the functionality of the 1-Na-PP1 towards the PKD3-M/G was tested. In fact, we did observe a significant increase of tetraploid- and a decrease of diploid population (figure 12) when the inhibitor was applied to the cells after starvation, with a greater respond from the cells treated with the highest concentration of PP1 (10μM). Thus, this was taken as a first evidence that an increased population within the cell pool tested are arrested in the M phase, and implicate that the applied inhibitor worked. Unfortunately, the PKD3$^{-/-}$ data in this experiment cannot serve as a proper control since they don't respond to the starvation. Thus, it is therefore difficult to make a final conclusion/statement regarding efficiency of the PP1 analog. However, we can clearly state that the inhibitor is specific for the gatekeeper construct, since no changes were observed for the WT.

Considering that the PKD3-M/G cell line performed better with a higher concentration of PP1-analog, compared to PKD1 gatekeeper constructs, might indicate that it is difficult to obtain the arrest in M phase. Since the proliferation of the PKD3-M/G is good, it might also be possible that the constant employment of the PKD3-M/G, which is fairly low expressed, reduces the efficiency of the inhibitor, leading to suboptimal inhibition at the time point when the samples were collected. Aiming to finalize this experiment, samples need to be collected at more time points and an even higher concentration of the PP1-analog should be tested. To obtain a better synchronization, different drugs should be tested, to select for a drug that doesn't disrupt the inhibitor. In addition, a longer incubation with the PP1 analog might slow down the proliferation, and also properly restore the deficient phenotype.

Furthermore, it can be predicted that the gatekeeper exchange to alanine also would rescue the deficient cells, since the glycine gatekeeper variant didn't affect the *in vivo* activity of the

kinase. However, since the alanine variant have less specificity towards the inhibitor, it is difficult to make any assumptions before it is functionally tested.

5.4 Future perspectives

We have successfully established both gatekeeper variants for PKD1, and will aim to complete the same set for PKD3.
Now that the tools have been successfully established, they can be used for further approaches. Two of these will be discussed in the further.

(i) During the general activation mechanism of PKDs, the ATP binding pocket gets exposed thus the 1-Na-PP1 inhibitor can access and inhibit the kinase. Since all PKD constructs are tagged with a GFP, the localization of PKD1 and PKD3 upon activation can be followed. Data obtained from this approach might be different from existing observations and possibly shed light onto the necessity of kinase activation for a specific intracellular localization. In addition, if we can establish were the kinases are localized upon activation, one can narrow down more precisely possible functions and signaling pathways.

(ii) Furthermore, a more precise substrate identification can be started. A –S labeled ATP, N6-(benzyl)ATP, have been designed, which have affinity towards analog sensitive kinases. This analog provides therefor direct substrate labeling, and an identification of thiophosphate labeled substrates could be done via mass spectrometry (MS). Unfortunately, all currently available –S labeled ATP are not able to enter the cell. Thus approaches employing this analog are based on *in vitro* kinase assays, which are suboptimal due to their artificial nature.
Another approach for a direct substrate identification would be the characterization of missing phosphorylated substrates in deficient cells by MS. MS measures the masses of small molecules by breaking them down to small ions and further sorting by their mass-to-charge ration, allowing for determination of the amino acid sequence of the peptide (Hirsch et al., 2004). Therefore, a MS would be able to recognize such a small difference as a phosphorylation of a substrate found in WT which has not been phosphorylated in the deficient cells. However, a complete knockout can influence phosphorylation events which might not be directly regulated by PKDs or represent an adaptation to the deficiency, which makes it difficult in the first place to distinguish direct substrates from the alternatives. Thus any results generated by this strategy needs to be verified by an alternative approach. So a general strategy to identify kinase substrates would be to identify missing phospho substrates in deficient material when compared

to wild type material, which then can be verified by using the gatekeeper mutation, expressed in the deficient background, in combination with the specific inhibitor.

The complexity of the content in a whole cell extraction might create a lot of background and also many false positives. Considering PKD1, we can as a starting point take advantage of its involvement in ROS-mediated responses, which is taking place at the mitochondria. To minimize false positives, a WT sample treated with enough H_2O_2 (e.g. 50 μM) to cause mitochondrial depolarization should be compared to an untreated WT control in the first place. This way, substrates giving the same profile for both samples, can be subtracted, since no changes indicate no involvement. Both the mitochondria fraction and the cytosolic fraction of the treated samples would be expected to have phosphorylated substrates not found in the untreated WT sample when compared via MS. However, the phosphorylated substrates found in the treated sample, does not necessarily indicate PKD1 involvement, but they might be apoptosis related substrates. Likewise, an equal comparison could be made between untreated and treated $PKD1^{-/-}$. Phosphorylated substrates in the treated (e.g. 25 μM H_2O_2) $PKD1^{-/-}$ sample (either characterized from the mitochondria fraction or cytosol), also found in the WT treated sample, would indicate that these substrates are not PKD1 dependent, and can therefore be excluded. After this last elimination step, we would have identified some possible substrates. The same experiment would then be repeated with the analog sensitive kinase, using $PKD1^{-/-}$ cells expressing exogenous PKD1 gatekeeper variant as WT, and the same analog sensitive cell line with inhibitor as the deficient control. For the latter experiment, it might be predicted that some phospho substrates found in the former experiment are missing and vice versa. Nevertheless, substrates identified with both approaches are most likely to be downstream targets in a PKD1 signal transduction pathway, with the possibility of being direct substrates. The identified substrates could then be further investigated for the possibility of being direct substrates, via e.g. PKD1 motif searching.

Since this described experiment regards PKD1, which might have anti-apoptotic substrates, the final goal would be to identify a specific substrate which can be used as a target protein in cancer, since inducing apoptosis in cancer under deprevation conditions is a good thing.

6 References

Asaoka Y, Nakamura S, Yoshida K, Nishizuka Y. 1992. Protein kinase C, calcium and phospholipid degradation. Trends Biochem Sci **17:**414-417.

Azam M, Seeliger MA, Gray NS, Kuriyan J, Daley GQ. 2008. Activation of tyrosine kinases by mutation of the gatekeeper threonine. Nat Struct Mol Biol **15:**1109-1118.

Bishop AC, Shokat KM. 1999. Acquisition of inhibitor-sensitive protein kinases through protein design. Pharmacol Ther **82:**337-346.

Boyer PD. 1998. Energy, life, and ATP. Biosci Rep **18:**97-117.

Chen J, Deng F, Singh SV, Wang QJ. 2008. Protein kinase D3 (PKD3) contributes to prostate cancer cell growth and survival through a PKCepsilon/PKD3 pathway downstream of Akt and ERK 1/2. Cancer Res **68:**3844-3853.

Durand S, Cimarelli A. 2011. The inside out of lentiviral vectors. Viruses **3:**132-159.

Fu Y, Rubin CS. 2011. Protein kinase D: coupling extracellular stimuli to the regulation of cell physiology. EMBO Rep **12:**785-796.

Gill GN, Garren LD. 1970. A cyclic-3',5'-adenosine monophosphate dependent protein kinase from the adrenal cortex: comparison with a cyclic AMP binding protein. Biochem Biophys Res Commun **39:**335-343.

Hirsch J, Hansen KC, Burlingame AL, Matthay MA. 2004. Proteomics: current techniques and potential applications to lung disease. Am J Physiol Lung Cell Mol Physiol **287:**L1-23.

Inoue M, Kishimoto A, Takai Y, Nishizuka Y. 1977. Studies on a cyclic nucleotide-independent protein kinase and its proenzyme in mammalian tissues. II. Proenzyme and its activation by calcium-dependent protease from rat brain. J Biol Chem **252:**7610-7616.

Jensen RT. 2002. Involvement of cholecystokinin/gastrin-related peptides and their receptors in clinical gastrointestinal disorders. Pharmacol Toxicol **91:**333-350.

Johannes FJ, Prestle J, Eis S, Oberhagemann P, Pfizenmaier K. 1994. PKCu is a novel, atypical member of the protein kinase C family. J Biol Chem **269:**6140-6148.

Kurian KM, Watson CJ, Wyllie AH. 2000. Retroviral vectors. Mol Pathol **53:**173-176.

Lindberg RA, Quinn AM, Hunter T. 1992. Dual-specificity protein kinases: will any hydroxyl do? Trends Biochem Sci **17:**114-119.

Liu Y, Bishop A, Witucki L, Kraybill B, Shimizu E, Tsien J, Ubersax J, Blethrow J, Morgan DO, Shokat KM. 1999. Structural basis for selective inhibition of Src family kinases by PP1. Chem Biol **6:**671-678.

Lopez MS, Kliegman JI, Shokat KM. 2014. The logic and design of analog-sensitive kinases and their small molecule inhibitors. Methods Enzymol **548:**189-213.

Nishizuka Y. 1995. Protein kinase C and lipid signaling for sustained cellular responses. FASEB J **9:**484-496.

Oeckinghaus A, Ghosh S. 2009. The NF-kappaB family of transcription factors and its regulation. Cold Spring Harb Perspect Biol **1:**a000034.

Ohno S, Nishizuka Y. 2002. Protein kinase C isotypes and their specific functions: prologue. J Biochem **132:**509-511.

Rey O, Yuan J, Rozengurt E. 2003a. Intracellular redistribution of protein kinase D2 in response to G-protein-coupled receptor agonists. Biochem Biophys Res Commun **302:**817-824.

Rey O, Yuan J, Young SH, Rozengurt E. 2003b. Protein kinase C nu/protein kinase D3 nuclear localization, catalytic activation, and intracellular redistribution in response to G protein-coupled receptor agonists. J Biol Chem **278:**23773-23785.

Roffey J, Rosse C, Linch M, Hibbert A, McDonald NQ, Parker PJ. 2009. Protein kinase C intervention: the state of play. Curr Opin Cell Biol **21:**268-279.

Roskoski R, Jr. 2015. A historical overview of protein kinases and their targeted small molecule inhibitors. Pharmacol Res **100:**1-23.

Rozengurt E, Rey O, Waldron RT. 2005. Protein kinase D signaling. J Biol Chem **280:**13205-13208.

Rozengurt E, Sinnett-Smith J, Van Lint J, Valverde AM. 1995. Protein kinase D (PKD): a novel target for diacylglycerol and phorbol esters. Mutat Res **333:**153-160.

Rubin CS, Rosen OM. 1975. Protein phosphorylation. Annu Rev Biochem **44:**831-887.

Stafford MJ, Watson SP, Pears CJ. 2003. PKD: a new protein kinase C-dependent pathway in platelets. Blood **101:**1392-1399.

Storz P, Doppler H, Toker A. 2005. Protein kinase D mediates mitochondrion-to-nucleus signaling and detoxification from mitochondrial reactive oxygen species. Mol Cell Biol **25:**8520-8530.

Storz P, Toker A. 2003. Protein kinase D mediates a stress-induced NF-kappaB activation and survival pathway. EMBO J **22:**109-120.

Sturany S, Van Lint J, Gilchrist A, Vandenheede JR, Adler G, Seufferlein T. 2002. Mechanism of activation of protein kinase D2(PKD2) by the CCK(B)/gastrin receptor. J Biol Chem **277:**29431-29436.

Takai Y, Kishimoto A, Inoue M, Nishizuka Y. 1977. Studies on a cyclic nucleotide-independent protein kinase and its proenzyme in mammalian tissues. I. Purification and characterization of an active enzyme from bovine cerebellum. J Biol Chem **252:**7603-7609.

Tuteja N. 2009. Signaling through G protein coupled receptors. Plant Signal Behav **4:**942-947.

Wang QJ. 2006. PKD at the crossroads of DAG and PKC signaling. Trends Pharmacol Sci **27:**317-323.

Xu X, Gera N, Li H, Yun M, Zhang L, Wang Y, Wang QJ, Jin T. 2015. GPCR-mediated PLCbetagamma/PKCbeta/PKD signaling pathway regulates the cofilin phosphatase slingshot 2 in neutrophil chemotaxis. Mol Biol Cell **26:**874-886.

Zanin E, Desai A, Poser I, Toyoda Y, Andree C, Moebius C, Bickle M, Conradt B, Piekny A, Oegema K. 2013. A conserved RhoGAP limits M phase contractility and coordinates with microtubule asters to confine RhoA during cytokinesis. Dev Cell **26:**496-510.

Zhang T, Sell P, Braun U, Leitges M. 2015. PKD1 protein is involved in reactive oxygen species-mediated mitochondrial depolarization in cooperation with protein kinase Cdelta (PKCdelta). J Biol Chem **290:**10472-10485.

Zugaza JL, Sinnett-Smith J, Van Lint J, Rozengurt E. 1996. Protein kinase D (PKD) activation in intact cells through a protein kinase C-dependent signal transduction pathway. EMBO J **15:**6220-6230.

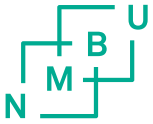

Norges miljø- og biovitenskapelig universitet
Noregs miljø- og biovitskapelege universitet
Norwegian University of Life Sciences

Postboks 5003
NO-1432 Ås
Norway